TECTONIC DEFORMATION OF THE ANDES AND THE CONFIGURATION OF THE SUBDUCTED SLAB IN CENTRAL PERU: RESULTS FROM A MICRO-SEISMIC EXPERIMENT

G. Suárez,[1,5], J. Gagnepain[2], A. Cisternas[2], D. Hatzfeld[3], P. Molnar[1], L. Ocola[4], S.W. Roecker[1] and J.P. Viode[2,6]

1) Department of Earth and Planetary Sciences
Massachusetts Institute of Technology
Cambridge, MA 02139 USA

2) Institut de Physique du Globe
Universite de Paris VI
4 Place Jussieu
75006 Paris, France

3) Laboratoire de Geophysique Interne, IRIGM
Universite Scientifique et Medicale de Grenoble
Saint Martin d'Heres, France

4) Instituto Geofísico del Perú
Lima, Peru

5) (present address) Lamont-Doherty Geological Observatory
Columbia University
Palisades, NY 10964 USA

6) Junior authors in alphabetical order

to G.J.R.a.S.

ABSTRACT

A microearthquake study was conducted in the central Andes of Peru, east of the city of Lima, to study the seismicity and style of tectonic deformation of the Peruvian Andes. Although most of the stations forming our temporary seismographic network were located on the high Andes, the vast majority of the microearthquakes recorded occurred to the east: on the Huaytapallana fault in the Eastern Cordillera or in the western margin of the sub-Andes. Thus, the sub-Andes appear to be the physiographic province subjected to the most intense seismic deformation. Focal depths for the crustal events in this region are as deep as 50 km, and the fault-plane solutions, as in the case of the teleseismic earthquakes, show thrust faulting on steep planes oriented roughly north-south. The Huaytapallana fault in the Cordillera Oriental also shows relatively high seismicity along a northeast-southwest trend that agrees with the fault scarp and the east-dipping nodal plane of two large earthquakes that occurred on this fault on July 24 and October 1, 1969. Microearthquakes of intermediate depth recorded during the experiment show a flat seismic zone about 25 km thick at a depth of about 100 km. This agrees with the suggestion that beneath Peru the slab first dips at an angle of 30° to a depth of 100 km and then flattens following a quasi-horizontal trajectory (Grange et al 1983, Hasegawa and Sacks 1981). Fault-plane solutions of intermediate-depth microearthquakes have horizontal T axes oriented east-west.

Introduction

The west coast of South America is the major active margin where an oceanic plate is being subducted beneath a continental plate. It represents a contemporary example of the tectonic regime that is often presumed to have existed along the western margin of North America before the subduction of oceanic material ceased during the late Cenozoic (e.g. Atwater 1970, Hamilton 1969). Thus, understanding the style of deformation and evolution of the Andes, an orogenic belt uncontaminated by a continental collision, may play a crucial role in trying to decipher the complex tectonic history of previously active margins that are now dormant, or where an "Andean" margin has been followed by a continental collision.

A useful tool to glean information about the style of deformation and tectonic regime of an active mountain belt is the study of the seismicity occurring in it. The spatial distribution of seismic activity indicates where brittle deformation is taking place, while the style of faulting inferred from fault-plane solutions allows inferences of the orientation of the stresses responsible for this deformation. In the Andes, crustal seismic activity is low compared to that of the subduction zone to the west, and the routine determination of hypocentral locations published by the International Seismological Centre (ISC) and the United States Geological Survey (USGS) are not accurate due both to the poor geographical distribution of stations at teleseismic distances and to the sparse coverage of the local stations; errors are specially large for focal depth determinations.

With the pupose of studying how the South American plate deforms due to the subduction of the Nazca plate to the west, and to understand in more detail the morpholgy of the subducted slab beneath central Peru we installed a temporary network of portable seismographs in the Altiplano and the Eastern

Cordillera of the central Andes, east of the city of Lima (Figure 1).

Methods of Analysis

From May 13 to June 12, 1980, we operated a network of up to sixteen portable seismographs complementing the less dense permanent seismic network operated by the Instituto Geofisico del Peru (Figure 1 and Table 1). Our goal was to monitor the seismic activity in the High Plateaus and the Eastern Cordillera in the vicinity of the city of Huancayo (Figure 1). The geographic coordinates and elevation above sea level of the portable stations were determined using topographical maps published by the Instituto Geografico Militar of Peru at a scale of 1:100,000 (Table 1). We estimate the uncertainty of the positions of the stations to be in the order of 250 meters.

We used Sprengnether MEQ-800 seismographs with Mark Products L4-C vertical seismometers. The amplifiers were generally set to 84 db, corresponding to a magnification of about 5×10^5 at 10 Hz. Earthquakes were recorded by a fine stylus on smoked paper at a speed of 60 mm/min. Records were changed every 48 hours and the drift of the internal clock of each instrument was checked at this same time interval, by directly recording time pulses transmitted by the WWV station in Colorado, USA. Clock drifts during these 48 hour periods were always less than 0.1 sec.

The arrival times of the phases of interest were digitized on a table-top digitizer. The accuracy of the readings depended on the level of background noise and the sharpness of the onsets. On the average we estimate an accuracy of about 0.1 seconds for P arrival times. S waves were also picked when they could be confidently identified, and we estimate the error in S wave arrival time to be in the order of 1 second.

The earthquakes were located using the computer program HYPOINVERSE developed at the USGS by Klein (1978). In the first iteration, P arrival times were assigned a weight of 1 and S arrival times a weight of 0.5. The smaller weights of the S waves compensate the larger uncertainty in arrival-time readings of S waves. The algorithm assigns weights to the observed arrival time as a function of the residual from the previous iteration. This is useful for damping arrival times that are grossly in error, as in the case of misidentified phases. Arrival times showing large residuals were reread.

A time correction (station delay) compensating for differences in elevation was applied to all arrival times at a given station. The station corrections were applied assuming a reference elevation of 3500 meters (the average elevation at the center of the array) and assuming a mean P-wave velocity of 5.0 km/sec for the top crustal layer.

Accuracy of the Locations

Effects of the Velocity Structure Utilized

The velocity structure in central Peru is poorly known. Although seismic refraction studies have been undertaken in southern Peru and northern Bolivia (e.g. Ocola et al 1971, Ocola and Meyer 1973, Tatel and Tuve 1958) little work has been done in central Peru to constrain the velocity structure there. To examine the uncertainties in our locations due to ignorance of the velocity structure, we calculated locations for selected events using three alternative velocity models (Table 2). The velocity structure inferred by Ocola and Meyer (1973) from a refraction survey across the Andes in southern Peru, that obtained by James (1971) from the dispersion of Rayleigh and Love waves along various paths in the Central Andes, and the velocity structure based on results of a deep crustal refraction experiment carried out in Colombia by Meissner et al (1977).

A random selection of 29 earthquakes occurring at various depths were located using these three seismic velocity structures. The difference in epicentral coordinates and focal depths of these 29 earthquakes located using the three alternative velocity models are shown in histogram form (Figure 2). In general, epicentral locations do not appear to depend strongly on the choice of the velocity structure; changes in epicentral coordinates are usually less than four to six kilometers. Focal depths, however, are more sensitive to changes in the velocity structure and may change by as much as 8 to 14 km depending upon the location of the event relative to the network. In both cases, however, those earthquakes that exhibited changes in epicentral coordinates larger than about 10 km are events that are poorly constrained because they lie outside or on the periphery of the network.

The velocity model obtained by Ocola and Meyer (1973) generally produced the smallest root-mean-square (rms) values of travel time residuals and was adopted to locate all the events recorded. A ratio of Vp/Vs of 1.73, corresponding to a Poisson's ratio of 0.25 was used in all cases. Other studies have shown that varying the ratio of Vp/Vs by about 0.3 produces changes in hypocentral locations that are usually not larger than 2 km (e.g. Chatelain et al 1980, Prevot et al 1980, Trehu 1982).

The Quality of Hypocentral Locations

As a result of the four weeks of recording a total of 344 earthquakes were located (Figure 3). The events located span an area of about 400 by 400 km. Most of these earthquakes occurred within the crust in the sub-Andes, east of the Andean Cordillera. Seismically, the high Andes appear to be relatively inactive with the exception of a linear northwest-southeast belt of earthquakes near the Huaytapallana fault in the Eastern Cordillera (near 12 S, 75 W). Intermediate-depth events were also located beneath the high Andes and the sub-Andes. Very

few events, however, were recorded along the main thrust contact between the Nazca and the South American plate possibly because this area is far from our network.

Many of the events lie outside the network and the maximum azimuthal gap in recording stations is sometimes quite large. A rule of thumb for judging the accuracy of hypocentral depth determination is that the distance from the event to the closest station should be less than or roughly equal to the focal depth. For most of the crustal earthquakes in the sub -Andes this is clearly not the case since many of them lie outside of our network. Focal depths of most of these crustal events appear to be less than 40 km and the distance to the closest station is often as large as 100 to 150 km. Consequently, HYPOINVERSE assigned large errors to the epicentral coordinates (ERH) and focal depths (ERZ) of many events located in the sub-Andes. Therefore, it is necessary to establish criteria for separating well located earthquakes from poor and unreliable locations. We consider as reliable locations those events for which a minimum of five arrival times, including at least one S phase, were used, those for which the calculated errors in the horizontal (ERH) and (ERZ) directions are less than 10 km, and earthquakes with rms travel-time residuals of less than 0.5 sec. The errors in the hypocentral parameters of earthquakes meeting these criteria are probably not larger than about 5 to 10 km. Among the 344 events that were located, only 114 events met these criteria (Figure 4).

Seismicity in the High Andes

Earthquakes in the Altiplano

It is clear that crustal seismicity in the Altiplano is relatively low (Figures 3, 4, and 5). Although the majority of our portable stations were deployed in the western part of the Altiplano, only about fifteen crustal earthquakes were

located beneath the network; the overwhelming majority of the crustal earthquakes occurred in the eastern margin of the Cordillera and in the sub-Andes (Figures 3 and 4). This pattern of seismicity is consistent with studies of teleseismic events showing that most large, shallow events occur in the western part of the sub-Andes (e.g. Stauder 1975, Suarez et al 1983). Thus, insofar as both the microearthquakes reported here and the historical seismicity reflect the degree of active tectonics, the Altiplano appears to be more stable and at present is not subjected to orogenic deformation as intense as that affecting parts of the Eastern Cordillera and the whole of the western sub-Andes. Otherwise, the deformation must either be episodic with large periods of quiescence or be absorbed by creep or viscoelastic behaviour.

Those few events that occurred in the Altiplano were all very small and their fault-plane solution could not be obtained. Thus, we could not address one of our original objectives: whether of not normal faulting occurs in the Altiplano of central Peru, as it does in the Cordillera Blanca of the high Andes in northern Peru (Dalmayrac 1974, Yonekura et al 1979) and in the Bolivian Altiplano (Lavenu 1978, Lavenu and Ballivian 1979, Mercier 1981).

The Huaytapallana Fault

The Huaytapallana fault is located in the Eastern Cordillera of central Peru, a few kilometers east of the city of Huancayo (Figure 1). Fault-plane solutions of two large earthquakes that occurred on this fault on July 24 and October 1, 1969 show reverse faulting (Stauder 1975). The earthquake on October 1 produced a steep fault scarp dipping east, with a vertical displacement reaching 1.6 m (Deza 1971, Philip and Megard 1977). Philip and Megard interpret the fault as one of a group of reactivated parallel faults trending NNW-SSE (Paredes 1972) (Figure 6).

The existence of a large number of small microearthquakes shows that the Huaytapallana fault (or system of faults) is still active (Figures 4 and 6). Station

HYT, installed at the southeastern end of the mapped surface rupture, registered an average of about 30 events per day with S-P time differences of less than 4 seconds. The epicenters of earthquakes located in the vicinity of the Huaytapallana area follow a trend in a NNW-SSE direction, parallel to the mapped surface faults and to the strike of the east-dipping nodal plane of the fault-plane solutions of the two larges Huaytapallana earthquakes (Stauder 1975, Suarez et al 1983) (Figure 6).

Both the fault-plane solution of one of the largest microearthquakes and a composite fault-plane solution for four other events show reverse faulting with some left lateral strike-slip motion occurring on a fault plane dipping east with a strike of about 30^0 west of north (Figure 7). This agrees with the sense of motion observed at the fault (Philip and Megard 1977) and with the fault-plane solution of the two large 1969 events.

In the basins just west of the Huaytapallana fault, Dollfus and Megard (1968) reported folding of Quaternary glacial morraines. The strike of these folds $N30^0W$ and the orientation of the P axes of the fault-plane solutions of earthquakes in the Huaytapallana fault (Figure 7) suggest this region is being deformed by a regional horizontal stress oriented roughly east-west, in the direction of plate motion.

Based on a study of the Huaytapallana fault scarp, Philip and Megard (1977) suggest that the overall length of the fault is approximately 3.5 km long. The length of the fault of the October 1, 1969 earthquake can be estimated by considering the average displacement u on the fault to be 1.6 m (Philip and Megard 1977), the rigidity μ equal to 3.3×10^{11}, a fault width of between 10 to 15 km, and a seismic moment, M_o, of 1.0×10^{26} dyne-cm (Suarez et al 1983). From the formula $M_o = \mu u S$ (Aki 1966), where S is the area of the fault, the October 1 earthquake requires a fault about 12 to 20 km long. Thus, it is likely that the 1969

event ruptured a fault that extends north of the surface break, to where the microearthquake activity occurs today. The epicenters of most of the earthquakes recorded in this area lie about 10 km east of the projected surface location of the fault (Figure 6).

A cross section across the fault shows that the depths of the earthquakes tend to increase towards the east (Figure 8), consistent with an east-dipping fault plane. The locations are not accurate enough to determine, however, whether the earthquakes take place on a single fault plane or on a series of imbricate faults.

Seismicity of the sub-Andes

Description of the Seismicity

The sub-Andes of central Peru are seismically more active than the high Andes and appear to be the physiographic province in the Peruvian Andes currently undergoing the most intense seismic deformation. The vast majority of earthquakes in the overriding continental plate are concentrated in the sub-Andean region over an area roughly 100 km wide. These events lie east of the main Andean Cordillera and occur beneath areas of low topographic elevation (Figures 3 and 4). Most of these events occurred at large distances from the eastern margin of the network and, therefore, the focal depths of these events are very poorly resolved. Station POC operated by the Instituto Geofisico del Peru is the only station located in the sub-Andes, but due to its low gain it could not be used to locate most of the microearthquakes that occurred in the area.

In the western part of the sub-Andes there are enough well located events to show that here the seismicity affects most of the crust, at least to depths of about 40 to 50 km, in agreement with the depths of two nearby teleseismic events (Chinn 1982, Suarez et al 1983). Although most of the microearthquakes

seem to occur at mid-crustal depths of between 15 and 25 km, one event clearly took place at a depth of 50 km. This earthquake occurred beneath the network and was located by 15 stations; the horizontal distance to the nearest station was about 30 km. Even though the travel-time residuals are relatively large (about 0.4 s), the estimated focal depth changes by less than 5 km for the different velocity models used, and the calculated errors in the vertical direction (ERZ) are always less than four kilometers. Below a depth of about 50 km there seem to be no earthquakes within the South American plate. An aseismic zone extends to a depth of about 90 km where intermediate-depth earthquakes associated with the subducted slab occur (Figure 5).

Fault-Plane Solutions and Tectonic Interpretation

A composite fault-plane solution from six events located just east of the network at depths of between 15 and 26 km shows thrust faulting with a component of strike-slip motion (Figure 9a). This solution is very similar to that of the larger May 15, 1976 event that occurred about 25 km east of this group of events at a depth of 20 km (Chinn 1982, Suarez et al 1983) (Figure 10). A fault-plane solution obtained for an event in the sub-Andes suggest nearly pure reverse faulting (Figure 9b). Both of these solutions have the P axes oriented northeast-southwest, in a direction perpendicular to the mountain range (Figure 10).

The existence of earthquakes in the sub-Andes at middle and lower crustal depths of between 20 and 50 km is unusual. In general, brittle deformation in the form of earthquakes is confined to the top 15 km of the crust (Chen and Molnar 1983, Meissner and Strelhau 1982). Below this depth, the absence of earthquakes is inferred to be due to the sharp decrease in strength of the typical crustal minerals at depth under normal geothermal gradients (e.g. Brace and Kohlstedt 1980, Caristan 1980). To explain both the concentration of intense deformation along the western margin of the sub-Andes and the unusually deep

seismic deformation of up to 40 or 50 km, Suarez et al (1983) suggested that the seismicity results from the underthrusting of the cold Brazilian shield beneath the eastern margin of the Cordillera Oriental.

It appears that the stresses applied to the western coast of the South American plate by the subduction of the Nazca plate are not elevating the Andean terranes that already have a high elevation. Instead, they seem to break and shorten the crust to the east where it is probably thinner. This crustal shortening would thicken the crust and uplift the topography of the eastern Cordillera causing the Andean mountain range to grow eastward. In this scenario, the relatively deep microearthquakes and the large teleseismic events in the western sub-Andes would reflect the tectonic deformation of the underthrust Brazilian shield (Suarez et al, 1983). The age and intensity of the sedimentary rocks in the sub Andes is generally shown to decrease progressively to the east (Dalmayrac et al 1980, Megard 1978) and may be interpreted as the result of the a detached wedge of sedimentary rocks lying east of the zone of intense deformation in the western sub Andes. The large number of shallow microearthquakes occurring in the sub Andes proper would then reflect the thin-skinned deformation of this accretionary prism.

Intermediate Depth Microearthquakes

Shape of the Subduction Zone beneath the Central Andes

Based on the study of a carefully selected catalog of teleseismically located events, Barazangi and Isacks (1976, 1979) inferred that the seismic zone dips at about 10° beneath Peru. As James (1978) pointed out, most of the events used by Barazangi and Isacks to infer this dip are shallow events along the coast or from a cluster of intermediate-depth earthquakes in northern Peru. Using earthquakes recorded by networks in southern Peru, Grange et al (1983) and

Hasegawa and Sacks (1981) inferred that the seismic zone beneath the northern part of their network dips at about 30° down to a depth of 100 km and then flattens. Because of the locations of their stations, neither study could confidently locate events more than 150 km from the coast to determine how far the seismic zone remains horizontal.

During our field investigation we located twenty intermediate-depth earthquakes ranging in depth from 85 to 110 km with uncertainties of less than about 10 km. These earthquakes seem to define a flat seismic zone about 25 km thick beneath the Andes and suggests that the seismic zone remains flat at a depth of about 100 km for at least a distance of 450 km from the trench (Figure 5). The slab does not seem to dip a constant slope of 15° as inferred by Barazangi and Isacks (1976, 1979). Very few events, however, were located on the main thrust contact between the Nazca and the South American plates and we were unable to constrain the dip of the initial portion of the subduction zone.

One of us (L. Ocola) prefers to interpret the seismicity as two slabs dipping at 30°; an active subduction zone along the western coast of South America and a now dormant and deeper one beneath the sub-Andes connected by a low dip "detachement" zone (Ocola, 1983).

Fault-Plane Solutions and the Continuity of the Slab

The fault-plane solutions determined for four of these intermediate -depth microearthquakes show normal faulting with T axes lying almost horizontally and parallel to the direction of relative plate motion (Figures 11 and 12).

The orientation of the T axes in the direction of the dip of the slab at intermediate depths in other subduction zones of the world has usually been interpreted as a result of the gravitational body force acting on the downgoing slab (Isacks and Molnar, 1969). If the intermediate part of the slab lies flat, however,

and it is decoupled from its deepest segment as suggested by the absence of earthquakes at depths of between 200 and 550 km in Peru, it is difficult to ascribe the horizontal T axes to gravitational body forces acting on the slab where the earthquakes occur.

Hasegawa and Sacks (1981) suggest that the horizontal T axes could be explained by a continous slab descending to a depth of 600 km with an aseismic portion between 200 and 550 km. Our results suggest that the seismic zone remains horizontal to a distance of about 650 km from the trench, where it appears to bend again and continue to greater depth with a relatively steep angle (Figure 13). This interpretation is supported by the presence of a cluster of intermediate-depth events occurring at depths of about 150 km beneath eastern Peru (see cross section B in Figure 3 of Barazangi and Isacks 1978). One could speculate that a large number of earthquakes occur here because of the stresses produced by the forces bending the slab, in a situation analogous to that of a plate bent at a trench.

It is unclear what could cause these contortions of the downgoing slab: the unbending of the plate to underplate the Andes horizontally over a distance of about 300 km, and the second change in dip thereafter (Figure 13). A possible culprit for this behaviour may be the buoyant nature of the Nazca ridge that resists subduction due to its lighter composition. Based on reconstructions of past plate motions, Pilger and Handshumacher (1981) suggest the Nazca and Tuamotu Ridges represent mirror images of hot-spot traces formed at the Pacific-Farallon plate boundary. The former resting on the Nazca plate and the latter on the Pacific plate. In order to be a mirror image of the Tuamotu Island Chain, the subducted eastern continuation of the Nazca Ridge must bend to the northeast and lie now beneath Peru (Pilger 1981). The buoyancy added to the slab by the ridge might induce the very shallow dip of the subduction zone in

this area. South of the Nazca Ridge, in southern Peru and northern Chile, the subducted slab does not have this positive buoyancy and the subduction process reverts to a steeper and more normal dip of about 30°. The more steeply dipping slab lying to the east of the flat seismic zone (Figure 13) may be interpreted as a remnant of a normal episode of plate subduction prior to the arrival of the easternmost extension of the Nazca Ridge to the trench.

Summary

A microseismic study of the Peruvian Andes east of the city of Lima was conducted during the summer of 1980 deploying a portable seismic network for three weeks. The seismicity reveals that the most intense seismic deformation of this portion of the Peruvian Andes occurs in the sub Andes. The majority of the microearthquakes located occur to the east of the high Andes beneath areas of low topographic relief. In the western margin of the sub Andes the seismicity reaches a depth of up to 50 km. The fault-plane solutions obtained for events in the western sub-Andes show high-angle reverse thrusting on planes oriented roughly north-south, in agreement with the orientation of the stresses expected from the direction of relative plate motion. The high Andes appear to be relatively aseismic suggesting that if they are being currently deformed by the stress that produces the high rate of seismicity in the sub Andes, the deformation is plastic and not brittle in nature. In the high Andes, only the Huaytapallana fault in the Eastern Cordillera shows a high rate of seismic activity. Here, the fault-plane solutions obtained from the microearthquakes are similar to those of the two large earthquakes that ruptured the fault in 1969. The microseismic activity in the vicinity of the Huaytapallana fault follows a trend parallel to mapped surface faults and the earthquakes become deeper from west to east suggesting an east-dipping fault plane. The intermediate depth events located range in depth from about 85 to 100 km. They define a flat seismic zone that underplates the Peruvian Andes horizontally up to a distance of 650 km from the trench. This is compatible with results obtained in southern Peru which suggest that beneath Peru the slab dips initially at an angle of about 30° down to a depth of 100 km and then flattens following a horizontal trajectory (Grange et al 1983, Hasegawa and Sacks 1981). The fault-plane solutions of the largest of these intermediate depth events show quasi-horizontal T axes oriented in the direction

of relative plate motion.

Acknowledgements

We thank R. Benites, A. Flores, and F. Pardo for ably assisting us in the field and D. Huaco, F. Megard, and M. Sebrier for their advice and help in logistics. We gratefully acknowledge the support provided by Ing. A. Giesecke, F. del Castillo, and J. Lanar at the Observatorio de Huancayo, Peru. This work was supported by NASA contract NAG5-300 and a grant from the Institut National d'Astronomie et de Geophysique.

REFERENCES

Aki, K., 1966. Generation and propagation of G waves from the Niigata earthquake of June 16, 1964, 2, Estimation of earthquake moment, released energy, and stress-strain drop from G wave spectrum, Bull. Earthquake Res. Inst. Tokyo, 44, 73-88.

Atwater, T., 1970. Implications of plate tectonics for the Cenozoic tectonic evolution of western North America, Geol. Soc. Amer. Bull., 81, 3513-3536.

Barazangi, M. & Isacks, B.L., 1976. Spatial distribution of earthquakes and subduction of the Nazca plate beneath South America, Geology, 4, 686-692.

Barazangi, M. & Isacks, B.L., 1979. Subduction of the Nazca plate beneath Peru: evidence from spatial distribution of earthquakes, Geophys. J. R. astr. Soc., 57, 537-555.

Brace, W.F. & Kohlstedt, D.L., 1980. Limits on lithospheric stress imposed by laboratory experiments, J. Geophys. Res., 85, 6248-6252.

Caristan, Y., 1982. The transition from high-temperature creep to fracture in Maryland diabase, J. Geophys. Res., 87, 6781-6790.

Chatelain, J.L., Roecker, S.W., Hatzfeld, D. & Molnar, P., 1980. Microearthquake seismicity and fault plane solutions in the Hindu Kush region and their tectonic implications, J. Geophys. Res., 85, 1365-1387.

Chen, W.P. & Molnar, P., 1983. Focal depths of intracontinental and intraplate earthquakes and their implications for the thermal and mechanical properties of the lithosphere, J. Geophys. Res., 88, 4183-4214.

Chinn, D.S., 1982. Accurate source depths and focal mechanisms of shallow earthquakes in western South America and in the New Hebrides island arc, Ph.D. Thesis, Cornell University, pp. 223.

Dalmayrac, B., 1974. Un example de tectonique vivante: les failles sub. actuelles du pied de la Cordillera Blanche (Perou), Cah. ORSTOM, Ser. Geol., 6, 19-27.

Dalmayrac, B., Laubacher, G. & Marocco, R., 1980. Geologie des Andes Peruviennes, Caracteres generaux de l'evolution geologique des Andes peruviennes, Travaux et Documents de l'ORSTOM, Editions de l'Office de la Recherche Scientifique et Technique Outre-Mer, Paris, France.

Deza, E., 1971. The Pariahuanca earthquakes, Huancayo, Peru: July-October 1969, in Recent Crustal Movements, R. Soc. N.Z. Bull., 9, 77-83.

Dollfus, O. & Megard, F., 1968. Les formations quaternaires du bassin de Huancayo et leur neotectonique (Andes centrales peruviennes), Rev. Geograph. Phys. Geol. Dynamique (2), X, 5, 429-440.

Grange, F., Cunningham, P., Gagnepain, J., Hatzfeld, D., Molnar, P., Ocola, L., Rodriguez, A., Roecker, S.W., Stock, J.M., and Suarez, G., 1983. The configuration of the seismic zone and the downgoing slab in southern Peru, submitted to Nature.

Hamilton, W., 1969. The volcanic central Andes - a modern model for the Cretaceous batholiths and tectonics of western North America, Oregon Dept. Geology and Mineral Industries, Bull., 65, 175-184.

Hasegawa, A. & Sacks, I.S., 1981. Subduction of the Nazca plate beneath Peru as determined from seismic observations, J. Geophys. Res., 4971-4980.

Isacks, B. & Molnar, P., 1969. Mantle earthquake mechanism and the sinking of the lithosphere, Nature, 223, 1121-1124.

James, D.E., 1971. Andean crustal and upper mantle structure, J. Geophys. Res., 76, 3246-3271.

James, D.E., 1978. Subduction of the Nazca plate beneath Central Peru, Geology, 7, 174-178.

Klein, F.W., 1978. Hypocenter location program Hypoinverse, Open-file report 78-694, United States Geological Survey, Menlo Park, 113pp.

Lavenu, A., 1978. Neotectonique des sediments plio-quaternaires du nord de l'Altiplano bolivien (Region de la Paz-Ayo-Ayo-Umala), Cah. O.R.S.T.O.M., ser. Geol., X, No. 1, 115-126.

Lavenu, A. & Ballivian, O., 1979. Estudios neotectonicos de las cuencas de las regiones de Cochabamba, Sucre, Tarija - Cordillera oriental boliviana, Rev. Acad. Nac. Cien. Bolivia. 2, No. 3. 107-129.

Megard, F., 1978. Etude geologique des Andes du Perou central, Office de la Recherche Scientifique et Tecnique Outre-Mer, Mem. 86, 310 pp.

Meissner, R. & Strehlau, J., 1982. Limits of stresses in continental crusts and their relation to the depth-frequency distribution of shallow earthquakes, Tectonics, 1, 73-89.

Mercier, J.L., 1981. Extensional-compressional tectonics associated with the Aegean Arc: comparison with the Andean Cordillera of south Peru-north Bolivia, Phil. Trans. R. Soc. Lond., 300, 337-355.

Ocola, L.C., Meyer, R.P. & Aldrich, L.T., 1971. Gross crustal structure under Peru-Bolivia Altiplano, Earthquake Notes, 42, 33-48.

Ocoa, L.C., Geophysical data and the Nazca-South America subduction zone kinematics: Peru-North Chile segment, in Geodynamics of the Eastern Pacific Region, Caribbean and Scotia Arcs, R. Cabre ed., Geodynamics Series vol. 9, A.G.U., Washington, D.C.

Ocola, L.C. & Meyer, R.P., 1973. Crustal structure from the Pacific basin to the Brazilian shield between 12° and 30° south latitude, Bull. Seism. Soc. Amer., 84, 3387-3403.

Paredes, J., 1972. Etude geologique de la feuille de Jauja au 1:100,000 (Andes du Perou Central), These 3eme Cycle, Univ. Sci. Tech. Languedoc, Montpellier, 79 pp.

Philip, H. & Megard, F., 1977. Structural analysis of the superficial deformation of the 1969 Pariahuanca earthquakes (central Peru), Tectonophys., 38, 259-278.

Pilger, R.H., 1981. Plate reconstructions, aseismic ridges, and low-angle subduction beneath the Andes, Geol. Soc. Amer. Bull., 92, 448-456.

Pilger, R.H. & Handschumacher, D.W., 1981. The fixed-hotspot hypothesis and origin of the Easter-Sala y Gomez-Nazca trace, Geol. Soc. Amer. Bull., 92, 437-446.

Prevot, R., Hatzfeld, D., Roecker, S.W. & Molnar, P., 1980. Shallow earthquakes and active tectonics in Eastern Afghanistan, J. Geophys. Res., 85, 1347-1357.

Stauder, W., 1975. Subduction of the Nazca plate under Peru as evidenced by focal mechanisms and by seismicity, J. Geophys. Res., 80, 1053-1064.

Suarez, G., Molnar, P. & Burchfiel, B.C., in press. Seismicity, fault-plane solutions, depth of faulting, and active tectonics of the central Andes, J. Geophys. Res.

Tatel, H.E. & Tuve, M.A., 1958. Seismic studies in the Andes, Amer. Geophys. Union Trans., 39, 580-582.

Trehu, A.M., 1982. Seismicity and structure of the Orozco transform fault from ocean bottom seismic observations, Ph.D. Thesis, Mass. Inst. of Tech. - Woods Hole Oceanographic Inst., 370 pp.

Yonekura, N., Matsuda, T., Nogami, M. & Kaizuka, S., 1979. An active fault along the western foot of the Cordillera Blanca, Peru, J. Geography, Tokyo, 88, 1-19.

TABLE 1

STATION COORDINATES

NAME	LAT	LONG	DELAY (sec)	LOCATION	ELEV (m)
ACO	-11.981	-75.095	0.08	ACOPALCA	3900
SAC	-11.778	-75.191	0.16	SACSACANCHA	4250
MAR	-11.604	-75.653	0.11	MARCAJASHA	4050
UNC	-11.235	-75.374	-0.36	UNCUSH	1925
COS	-12.140	-75.562	0.23	COSMOS	4600
CUL	-12.203	-75.211	0.06	CULHUAS	3800
LAI	-12.308	-75.359	0.07	LAIVE	3850
PAC	-11.778	-75.727	0.03	PACHACAYO II	3700
HYT	-11.960	-75.039	0.23	HUAYTAPALLANA	4600
PAM	-12.435	-74.870	0.04	PAMPAS	3750
PAG	-12.003	-74.917	0.01	PAGUA	3600
ATO	-12.341	-75.087	0.08	ATOMPAMPA	3900
MOL	-11.726	-75.409	0.02	MOLINOS	3650
PAR	-11.666	-75.085	0.12	PARCO II	3000
COC	-11.890	-75.305	-0.01	CONCEPCION	3500
COM	-11.699	-75.082	-0.12	COMAS	3000
YAU	-11.714	-75.469	-0.02	YAULI	3450
PA1	-11.782	-75.721	-0.03	PACHACAYO I	3700
PR1	-11.672	-75.083	-0.12	PARCO I	3000
VIS	-12.592	-74.961	0.12	VISCAPATA	4100
CHA	-12.011	-75.374	0.00	CHAMBARA	3350
GUA	-13.993	-75.789	-0.64	GUADALUPE	678
CAL	-12.627	-75.978	-0.42	CALACOCHA	1655
QUI	-12.943	-76.437	-0.68	QUILMANA	510
SJU	-15.356	-75.189	-0.77	SAN JUAN	75
NNA	-11.998	-76.843	-0.67	NANA	555
LM2	-12.068	-77.033	-0.67	LIMA2	127
HUA	-12.038	-75.323	-0.05	HUANCAYO	3313
VES	-12.213	-76.937	-0.77	V.EL SALVADOR	110
ANC	-11.775	-77.150	-0.78	ANCON	56
AYA	-13.080	-74.250	-0.17	AYACUCHO	2800
POC	-11.250	-74.600	-0.63	PTO OCOPA	750

TABLE 2

VELOCITY MODELS

Ocola and Meyer (1975)

Vp (km/sec)	Depth to layer (km)
5.0	0.0
5.6	10.0
6.0	22.0
7.9	65.0
8.0	100.0

Meissner et al (1977)

Vp (km/sec)	Depth to layer (km)
5.9	0.0
6.2	10.0
6.7	30.0
8.1	50.0

James (1970)

Vp (km/sec)	Depth to layer (km)
5.0	0.0
6.0	8.0
6.6	25.0
7.9	60.0
8.0	100.0

Figure Captions

Figure 1. Main physiographic units of the central Andes of Peru (after Megard 1978). Symbols show the location of the seismographic stations; filled symbols are the stations of the permanent Peruvian Network.

Figure 2. a) Histograms showing changes in calculated epicenters and focal depths for 29 events using the velocity structures proposed by Ocola and Meyer (1973) and James (1971) for the Central Andes.

b) Changes in calculated epicenters and focal depths for the same events using the velocity structures proposed by Ocola and Meyer (1973) for southern Peru and by Meissner et. al. (1977) for southern Colombia.

Figure 3. Epicenters of all 344 earthquakes recorded during the field experiment. Crosses indicate calculated depths shallower than 50 km and the triangles events deeper than 50 km. Closed symbols show locations of stations used to locate the earthquakes. Dashed lines show the 1000 and 3000 meter topographic contours of the central Andes.

Figure 4. Epicenters of screened catalog of well located microearthquakes. Symbols as in Figure 5.

Figure 5. Hypocenters of screened microearthquakes shown in Figure 6 projected on the cross section A-B. Vertical lines show the projected positions of the stations.

Figure 6. Epicenters of shallow events in the vicinity of the Huaytapallana fault plotted on a geological sketch-map of the Eastern Cordillera (after Philip and Megard 1977). Closed circles show epicenters and filled diamonds the seismic stations. Stars are the epicentral locations of the July 24 and October 1, 1969 earthquakes given by the ISC.

Figure 7. a) Composite fault-plane solution of four earthquakes b) Solution for single event located near the Huaytapallana fault, and c) Fault-plane solution for the July 24, 1969 earthquakes (Suarez et. al. 1983). These are lower-hemisphere equal-area projection. Open symbols indicate dilatation and closed symbols compression.

Figure 8. Hypocenters of the events shown in Figure 6 projected onto cross section A-B (Figure 6). Arrows indicate the positions of the stations and the dashed line is the assumed dip of the Huaytapallana fault from the fault-plane solution of the 1969 events (Stauder 1975).

Figure 9. a) Comparison of the composite fault-plane solution for six events in the sub-Andes and the fault-plane solution of the May 15, 1976 earthquake (Suarez et. al. 1983) that was located about 20 km east of the events used in the composite solution.

b) Fault-plane solution of an earthquake located in the western sub-Andes. Symbols as in Figure 9.

Figure 10. Map of the central Andes summarizing lower hemispheric projections of fault-plane solutions of shallow crustal events obtained in this study. Dark areas represent quadrants of compressional first motion. Numbers near fault-plane sulutions correspond to event numbers in Figure 7 and 9. Also shown are the fault-plane solutions of two large events (stars) studied by Suarez et. al. (1983) in this area.

Figure 11. Fault-plane solutions for four intermediate-depth events recorded in this study. Note T axes are nearly horizontal and oriented roughly east-west in all cases.

Figure 12. Map of central Peru summarizing lower hemisphere projections of the fault plane-solutions of intermediate-depth earthquakes obtained in this study. Numbers near fault-plane solutions correspond to event numbers shown in Figure 11. Shown as stars are the locations and faultplane solutions of the intermediate-depth events studied by Stauder (1975). Dark areas indicate quadrants of compressional first motions.

Figure 13. Cross section showing the inferred geometry of the subducted slab beneath Peru. To the earthquakes located in this study (shown as circles) we have added the best located intermediate-depth events selected by Barazangi and Isacks (1976) in Peru shown as squares). T axes of intermediate-depth events in this area are shown as arrows.

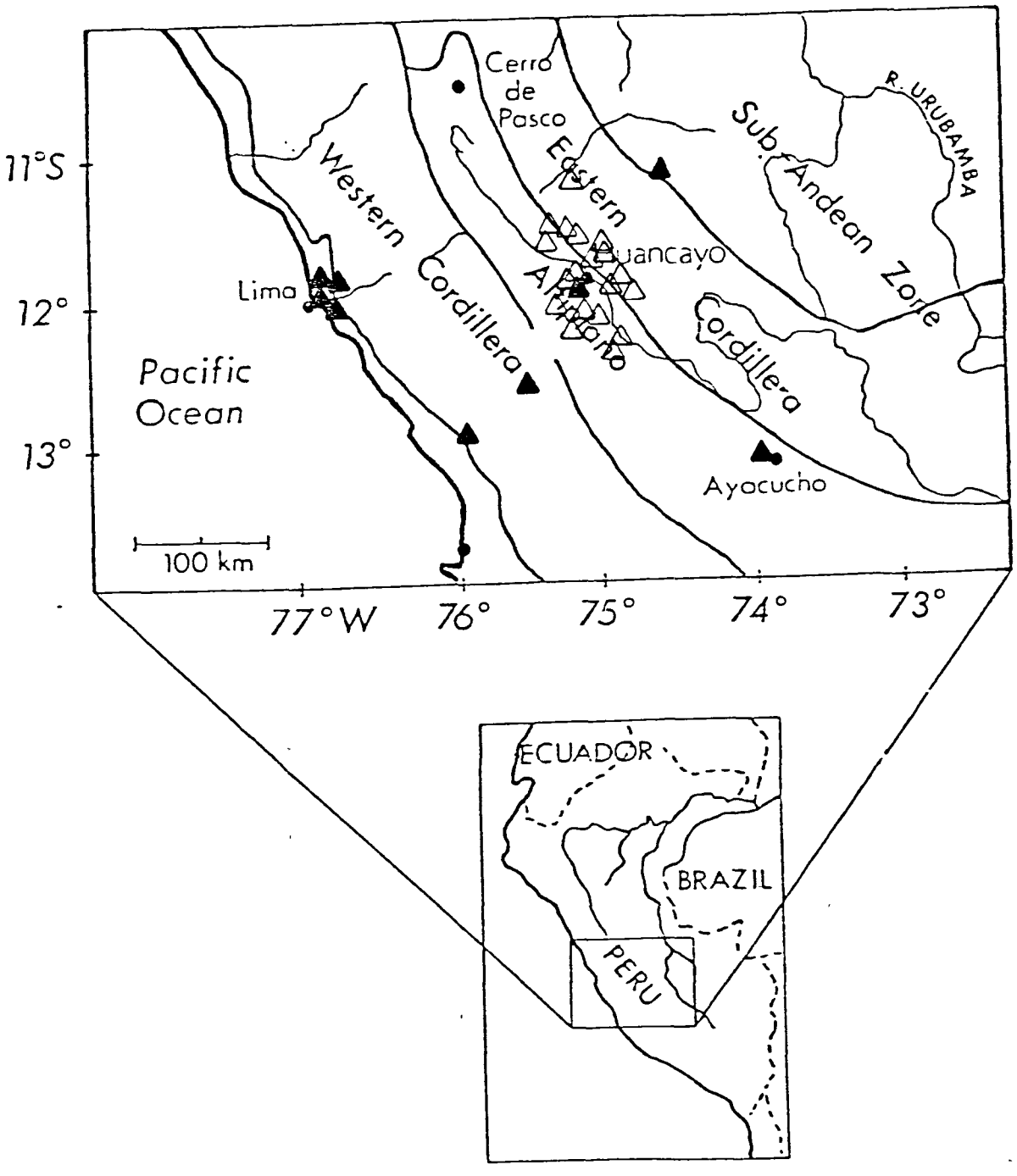
Cerro
de
Pasco
Western
Cordillera
Eastern
Cordillera
Sub-Andean Zone
R. URUBAMBA
Huancayo
Lima
Pacific
Ocean
Ayacucho
11°S
12°
13°
100 km
77°W
76°
75°
74°
73°
ECUADOR
BRAZIL
PERU

Figure 1

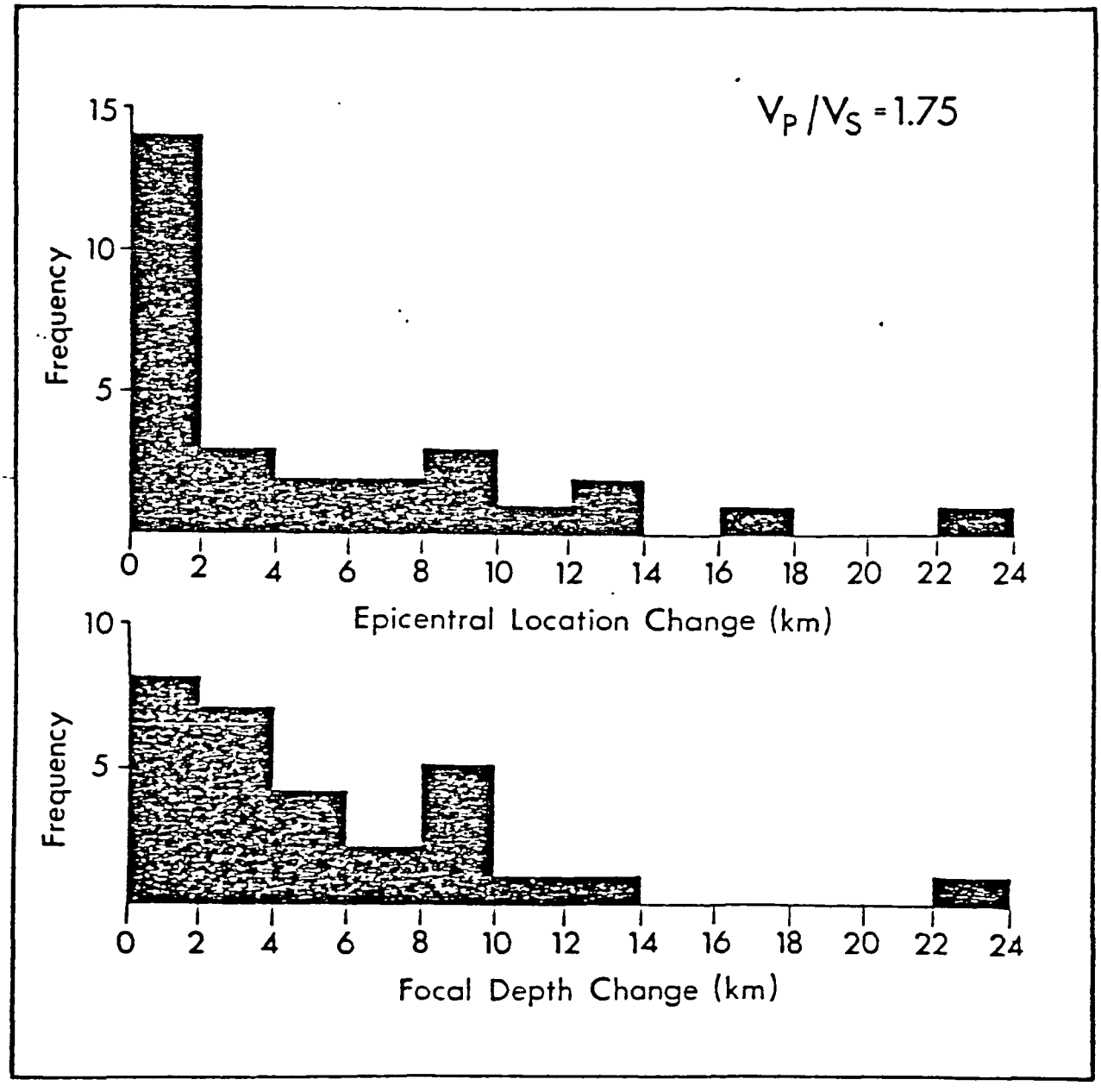
$V_P / V_S = 1.75$
Frequency
15
10
5
0 2 4 6 8 10 12 14 16 18 20 22 24
Epicentral Location Change (km)
Frequency
10
5
0 2 4 6 8 10 12 14 16 18 20 22 24
Focal Depth Change (km)

Figure 2a

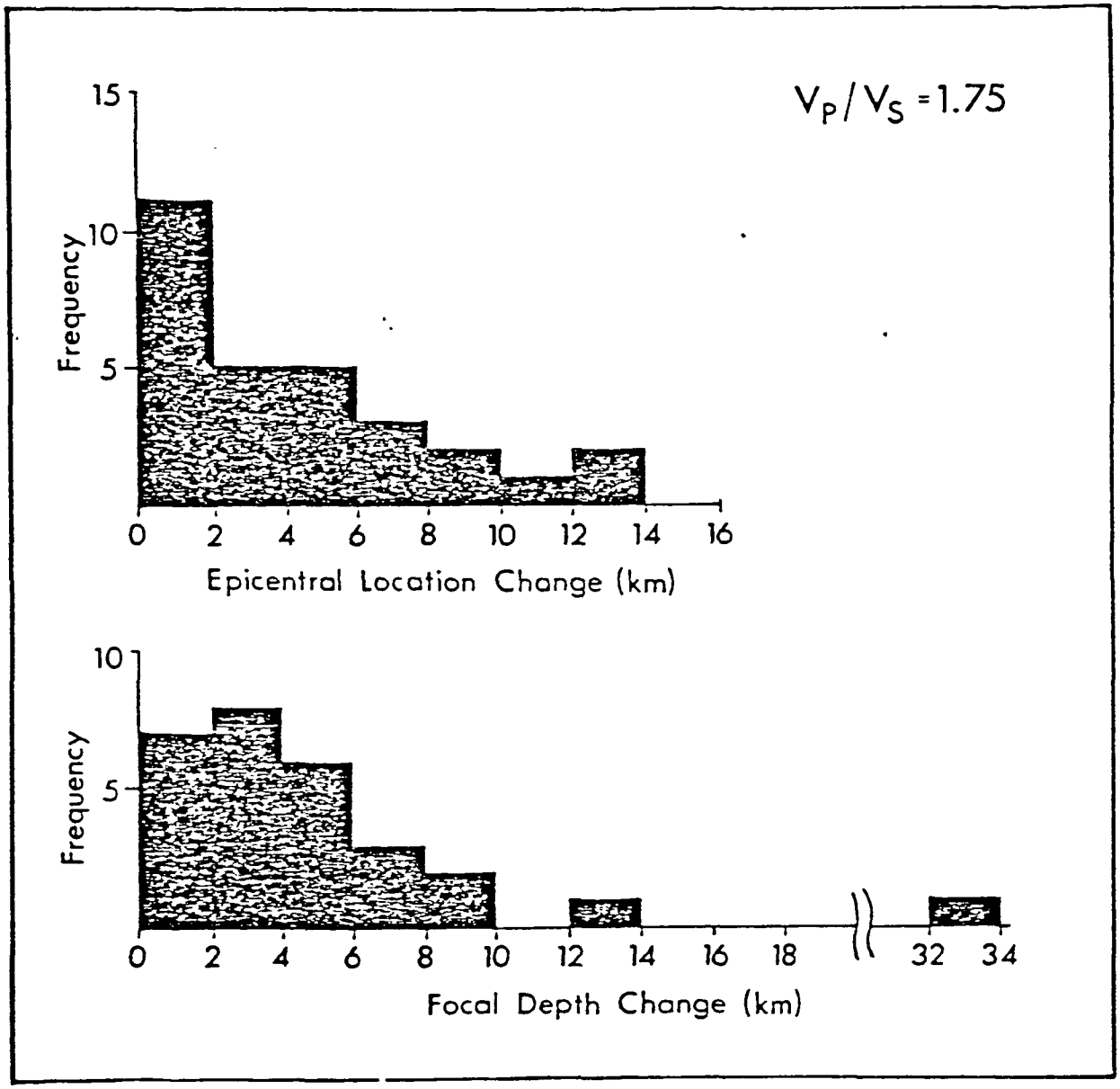
$V_P / V_S = 1.75$
15
10
5
Frequency
0 2 4 6 8 10 12 14 16
Epicentral Location Change (km)
10
5
Frequency
0 2 4 6 8 10 12 14 16 18 32 34
Focal Depth Change (km)

Figure 2b

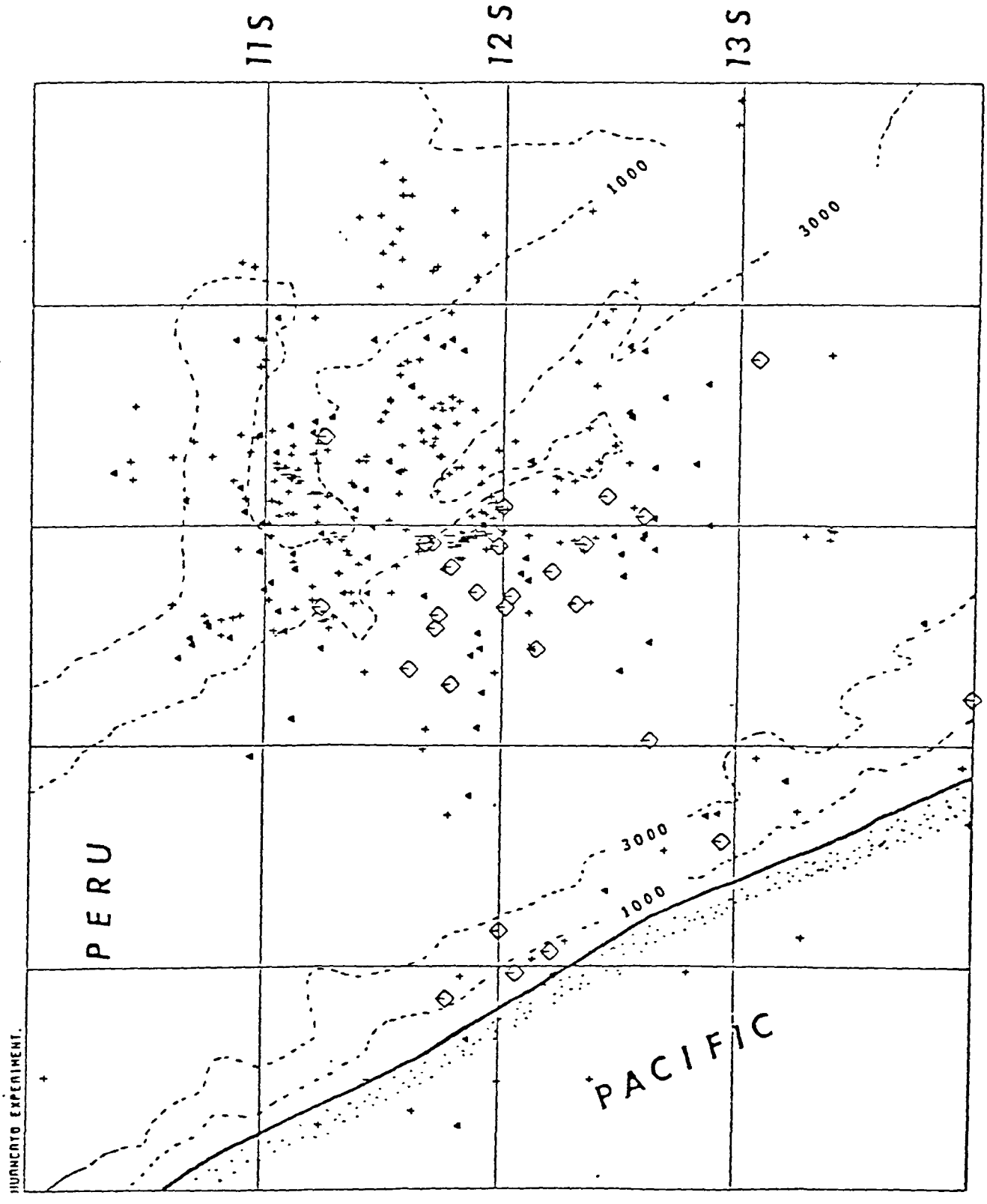
11S
12S
13S
1000
3000
3000
1000
PERU
PACIFIC
75W
77W
HUANCAYO EXPERIMENT.

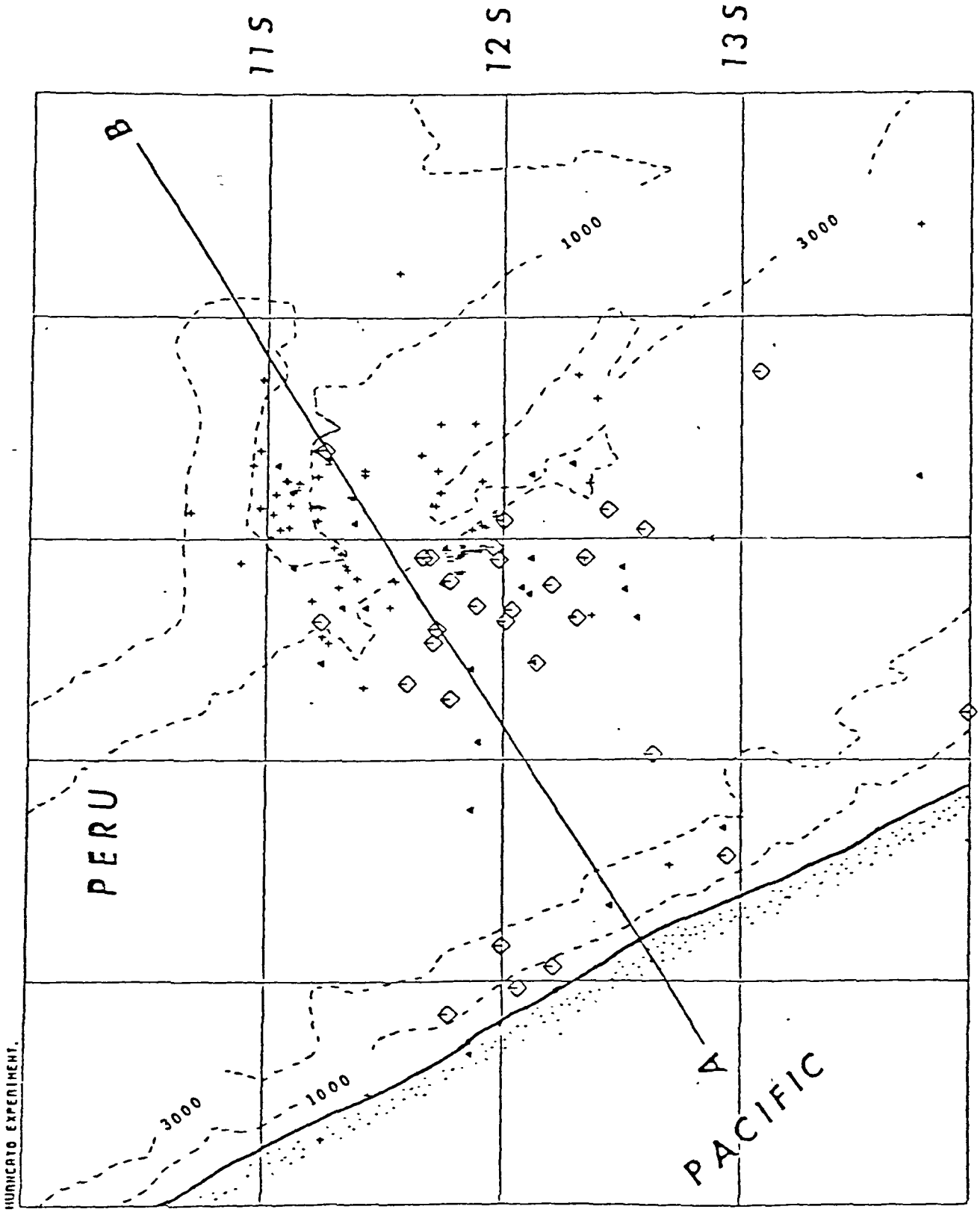
11 S
12 S
13 S
B
A
1000
3000
1000
3000
PERU
PACIFIC
75 W
77 W
HUANCAYO EXPERIMENT.

Figure 4

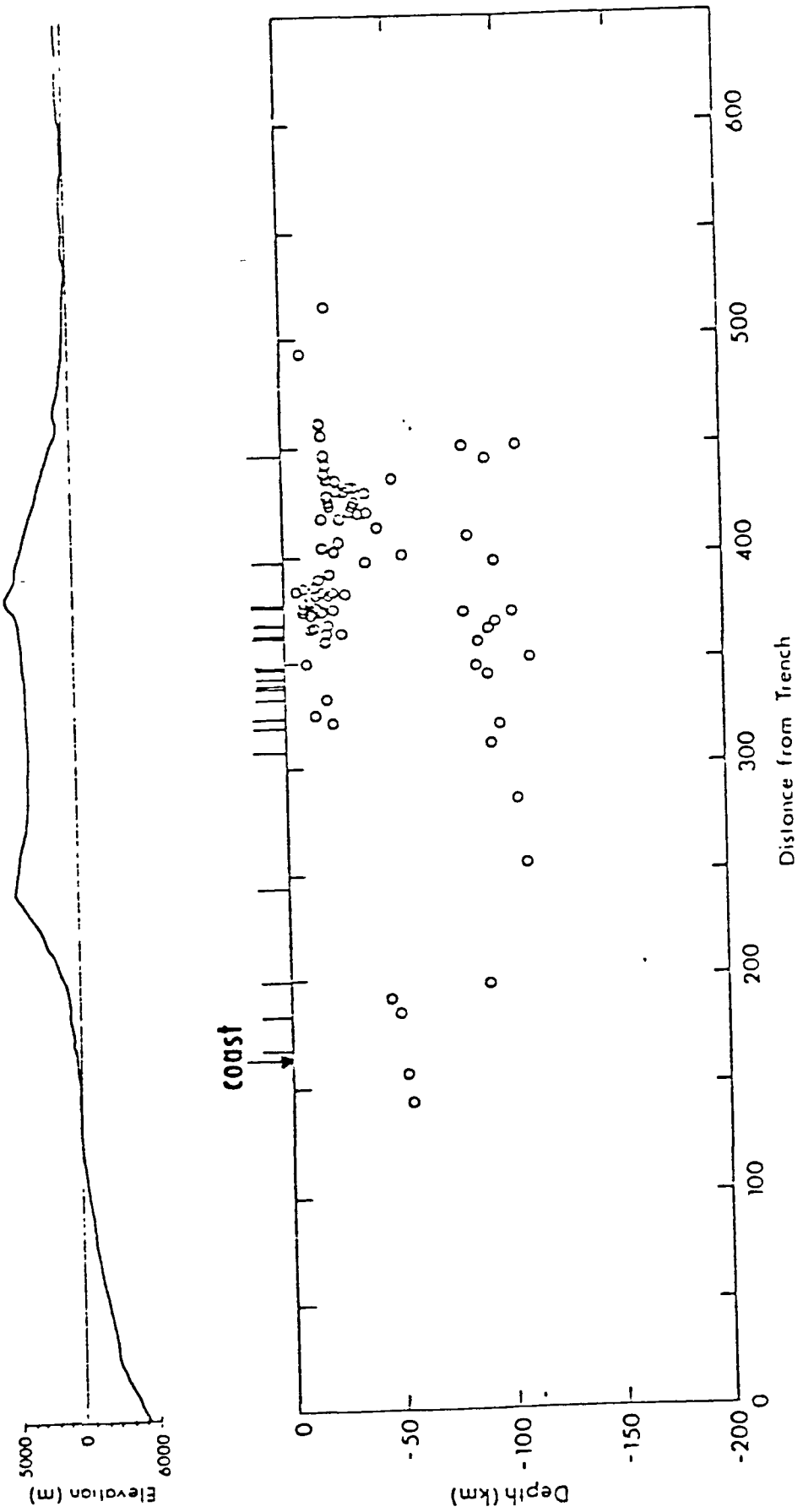
coast
Depth (km)
0
-50
-100
-150
-200
0
100
200
300
400
500
600
Distance from Trench
Elevation (m)
5000
0
6000

Figure 5

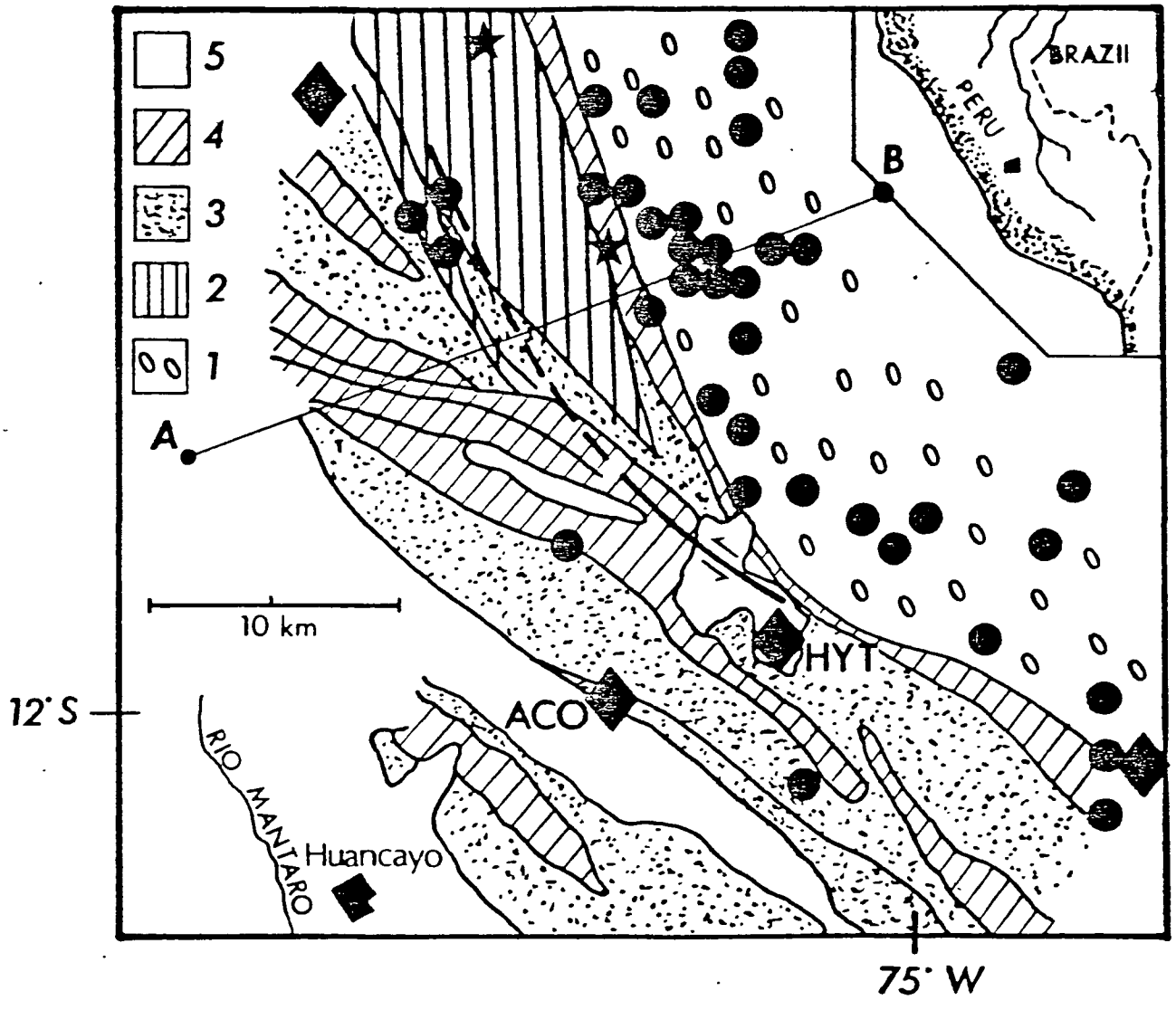
5
4
3
2
1
A
B
BRAZIL
PERU
10 km
HYT
ACO
12°S
RIO MANTARO
Huancayo
75°W

Figure 6

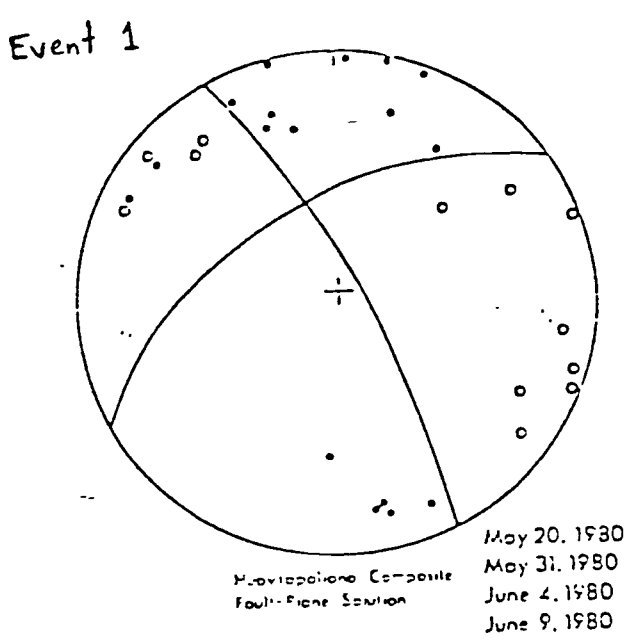
Event 1
May 20, 1980
May 31, 1980
June 4, 1980
June 9, 1980

(a)

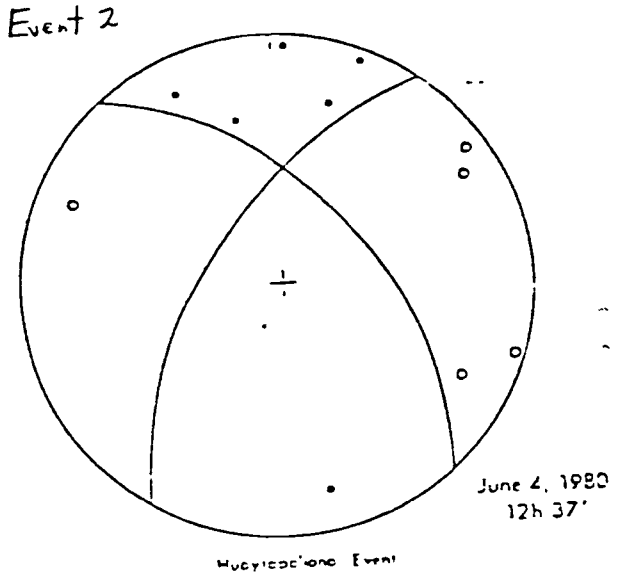
Event 2
June 4, 1980
12h 37'

(b)

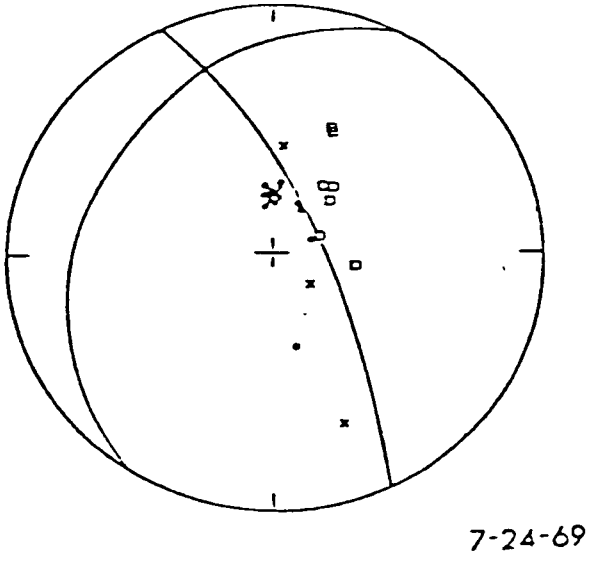
7-24-69

(c)

Figure 7

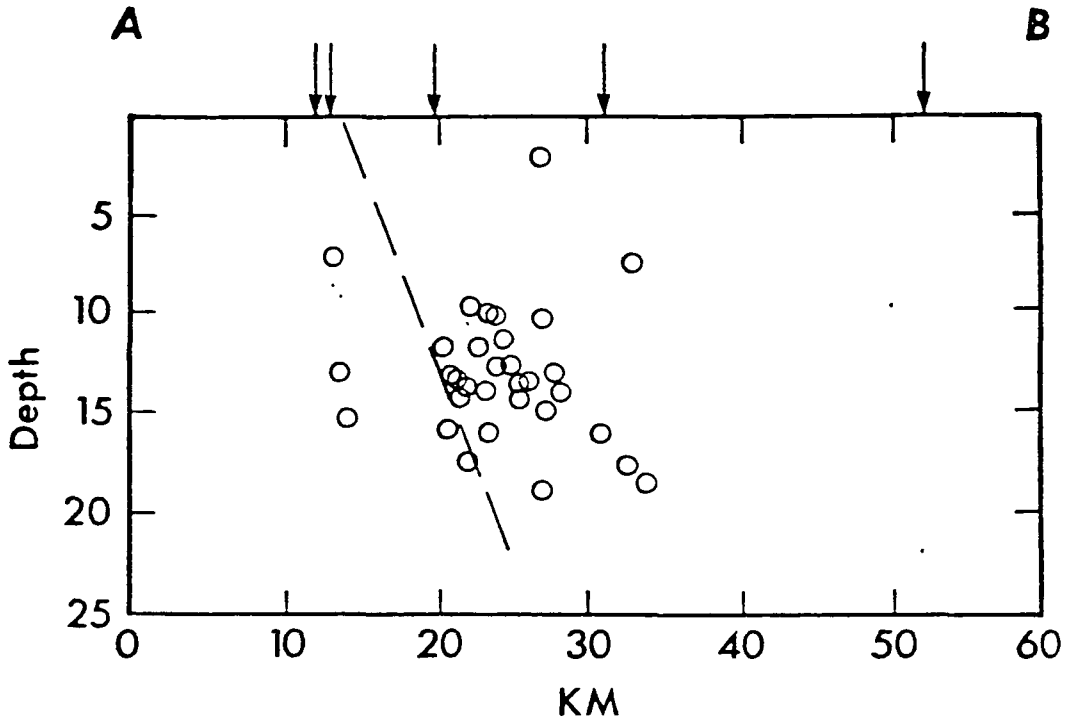

Figure 8

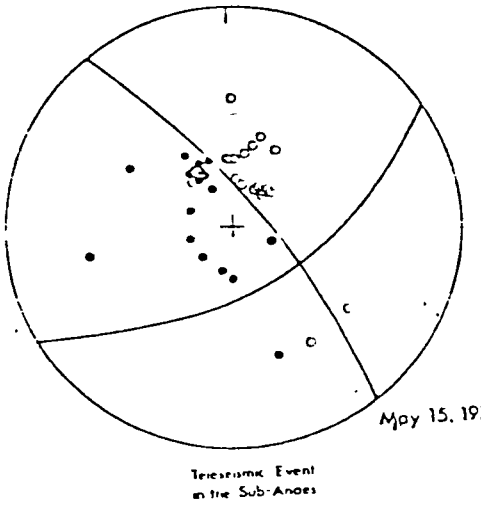

Event 3

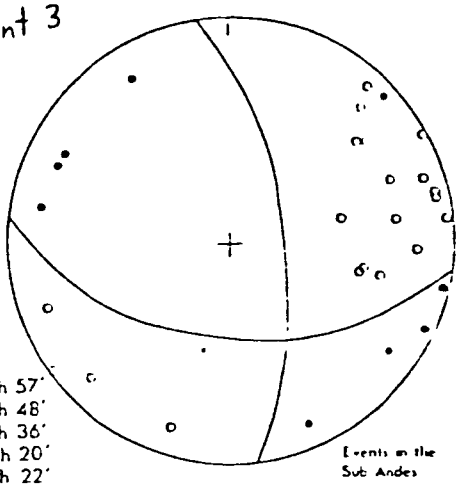

May 15 1980 7h 57'
May 20, 1980 2h 48'
May 24 1980 7h 36'
May 25 1980 23h 20'
June 4 1980 6h 22'
June 7, 1980 5h 07'

a)

Event 4

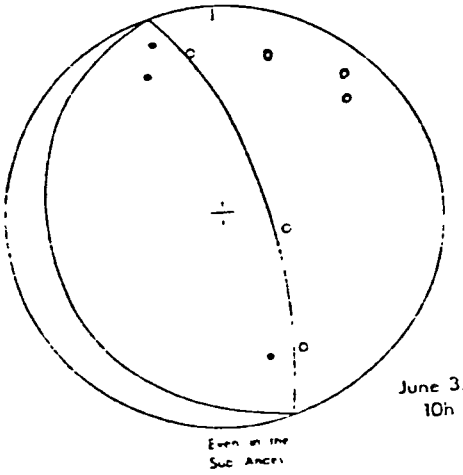

b)

Figure 9

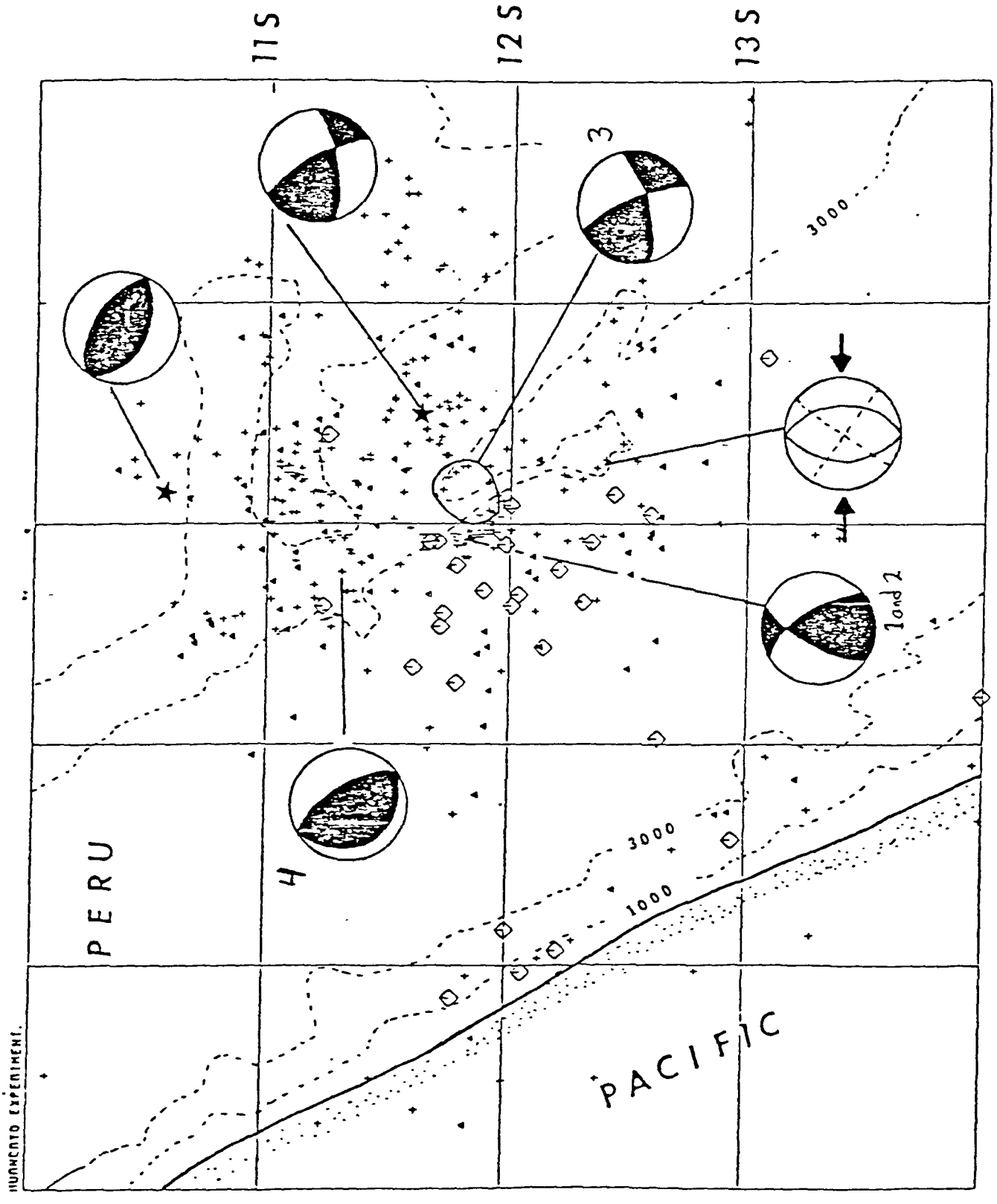

Figure 10

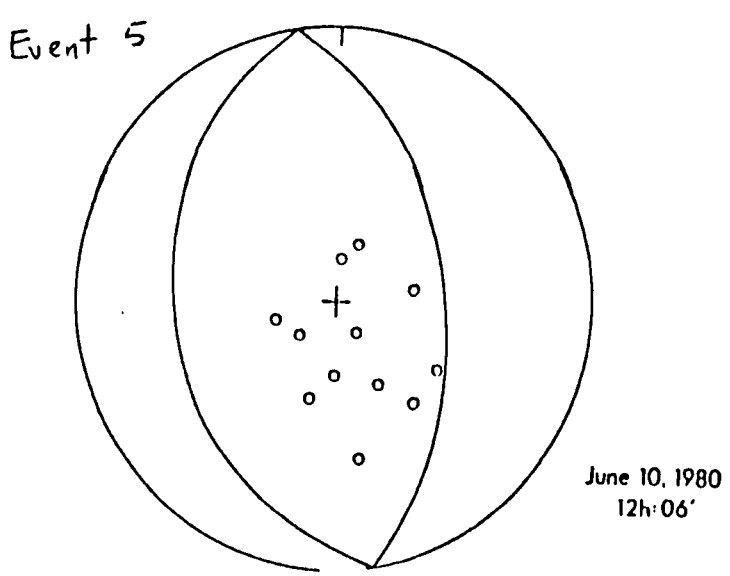
Event 5
June 10, 1980
12h:06'

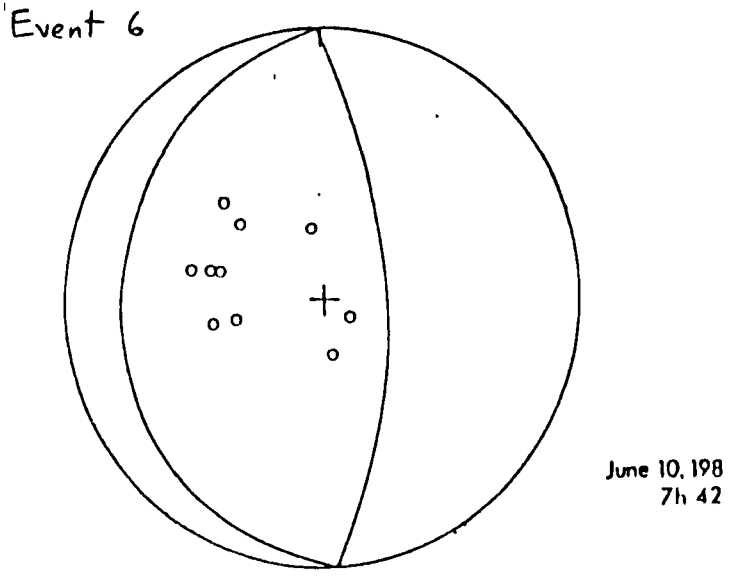
Event 6
June 10, 198
7h 42

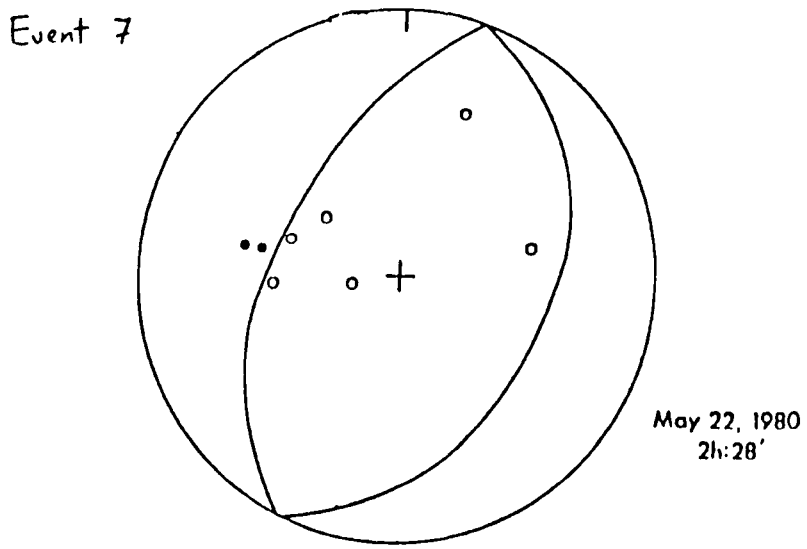
Event 7
May 22, 1980
2h:28'

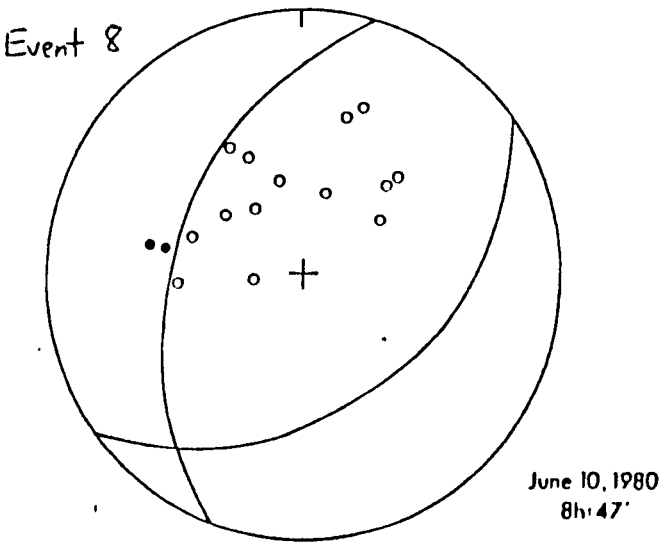
Event 8
June 10, 1980
8h:47'

Figure 11

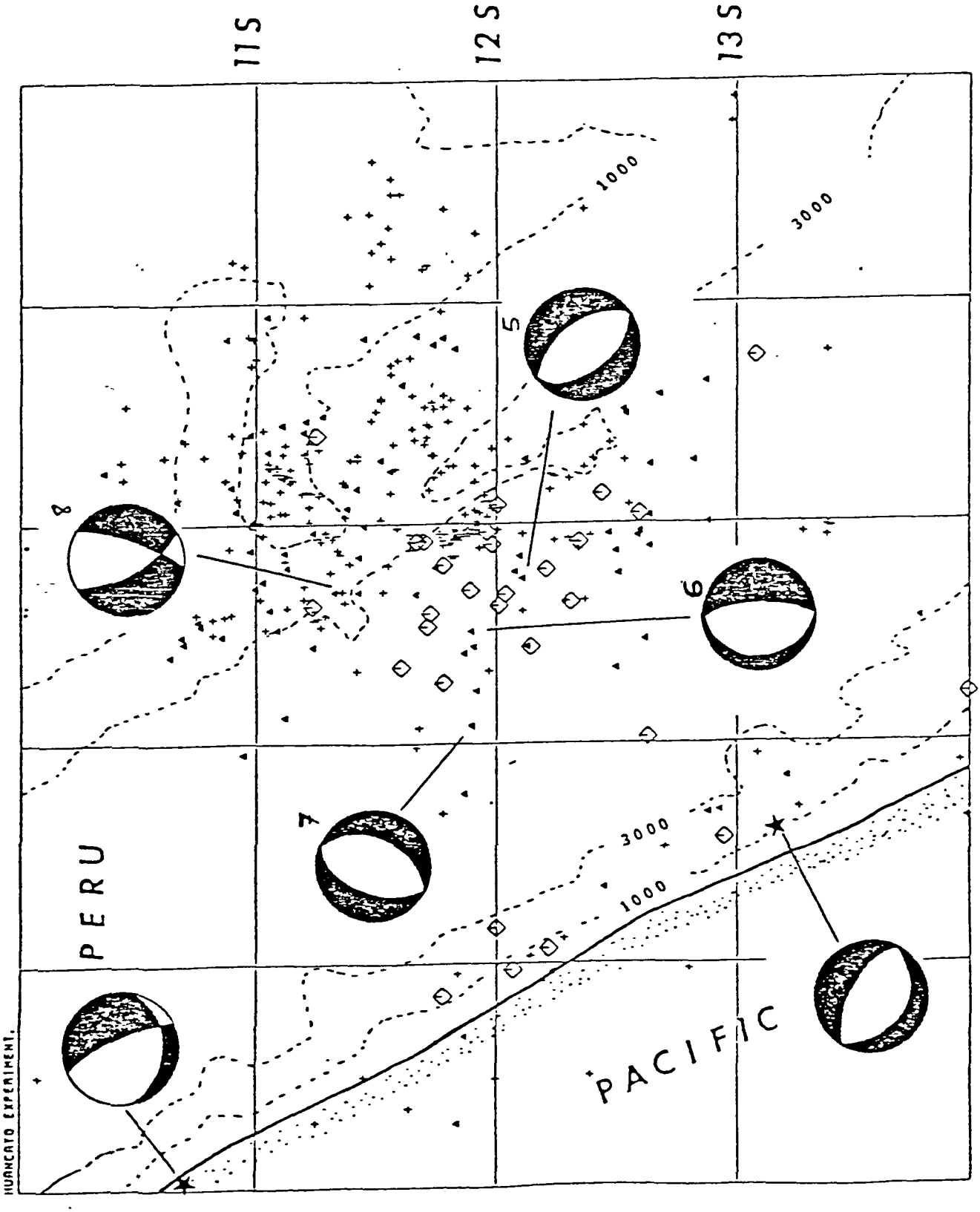
11 S
12 S
13 S
75 W
77 W
1000
3000
5
6
7
8
PERU
PACIFIC
HUANCAYO EXPERIMENT.

Figure 12

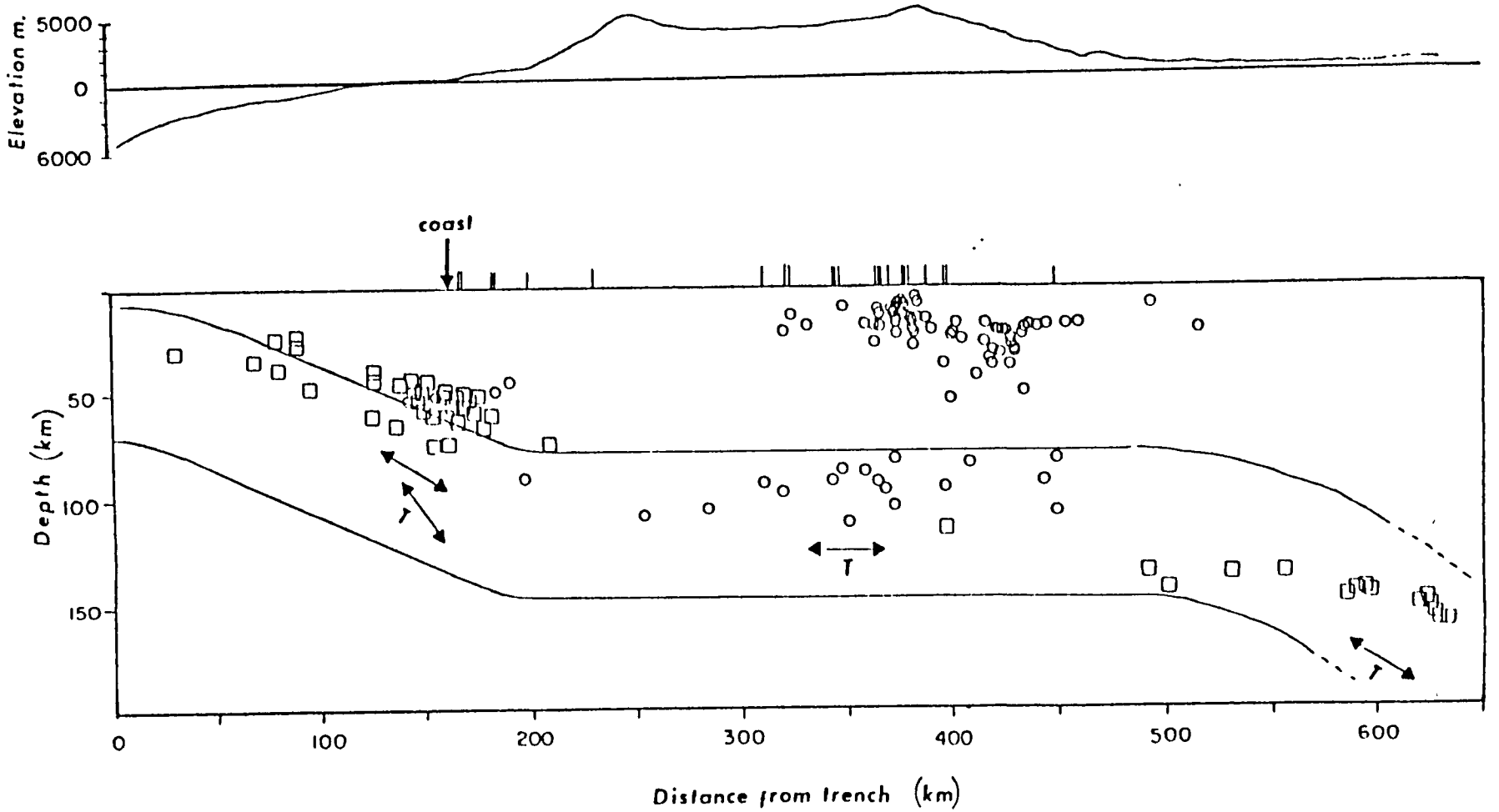
Elevation m.
5000
0
6000
coast
Depth (km)
50
100
150
T
T
T
0
100
200
300
400
500
600
Distance from trench (km)

Figure 13